**Zeitschrift:** IABSE reports of the working commissions = Rapports des commissions de travail AIPC = IVBH Berichte der Arbeitskommissionen

**Band:** 16 (1974)

**Artikel:** Large deformation and stability analysis of reinfroced concrete frames considering material nonlinearities

**Autor:** Aldstedt, E. / Bergan, P.G.

**DOI:** https://doi.org/10.5169/seals-15721

# Large Deformation and Stability Analysis of Reinforced Concrete Frames Considering Material Nonlinearities

Calcul des grandes déformations et de la stabilité des cadres en béton armé, tenant compte des comportements non-linéaires du matériau

Berechnung grosser Deformationen und der Stabilität von Stahlbetonrahmen unter Berücksichtigung der Nichtlinearitäten des Materials

E. ALDSTEDT
Research Fellow

P.G. BERGAN
Associate Professor of Civil Engineering

The Norwegian Institute of Technology
The University of Trondheim
Trondheim-NTH, Norway

## Introduction

It is widely recognized that the true behavior of reinforced concrete is extremely complicated. Among the various physical phenomena that occur on a macro-scopic level in reinforced concrete, the following will be mentioned: nonlinear compressive stress-strain relationship of concrete; cracking of concrete; yielding of steel reinforcement bars; bond slip between reinforcement bars and concrete. Geometric imperfections and second-order geometric effects are also of considerable importance for beam, plate and shell structures. The picture is further complicated by various time dependent phenomena. In spite all of this, the analyses of most concrete structures today are based on greatly simplified models for the materials.

The finite element method has proved to be a very efficient tool for analysis of a great variety of nonlinear problems [1], [2]. A review of applications of the method to nonlinear analysis of concrete structures has been given by Scordelis [3]. Studies considering both material nonlinearities and large deformations have previously been reported by Berg et.al. [4] who analyzed concrete plates and by Blaauwendraad [5] and Aas-Jakobsen and Grenacher [6] who dealt with concrete frames.

In theory, the finite element method can be formulated so that almost an unlimited number of complex physical and geometrical effects may be incorporated in the numerical algorithms. A prerequisite for this is of course that the various effects can be defined mathematically. But at least as important as to include various physical phenomena in the analytical model is to ensure that the method becomes economical and practical in use.

In the present paper an attempt is made to achieve a method of analysis that is capable of accurately predicting the inplane behavior of plane, slender, reinforced concrete frames and arches that are subjected to loads up to the ultimate carrying capacity. Major efforts have been made to make the analytical model economical and efficient. The approach is based on the finite element method utilizing a beam displacement model. The material properties of concrete and steel reinforcement may be relatively general. The loading , geometry, support conditions and distribution of reinforcement may also be arbitrary. The cross-sections are assumed to be rectangular. Large deflections of the frame are also accounted for. The present method is demonstrated by two numerical examples, eccentric buckling of a column and stability analysis of an arch.

## Governing equations

In the proceeding, a simple but powerful approach for large displacement analysis of frames will be followed. The structure is assumed to be divided into finite elements. To every element is "attached" a local Cartesian coordinate system going through the end nodal points, see Fig. 1.

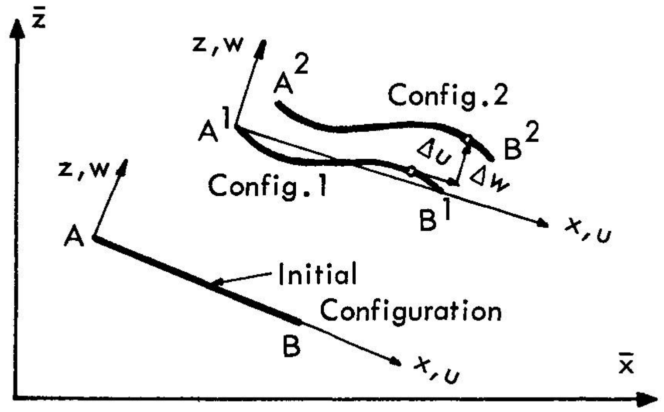


Fig.1. Description of motion of an element during deformation.

This coordinate system follows the element during the deformation. On the local element level the deformations are assumed to be small (small strains). However, forces and displacements for each element are transformed to a global coordinate frame in which the equilibrium equations for the entire system are assembled. In effect, this approach is a matter of updating the nodal point geometry of the structure in accordance with the current deformations. The geometric nonlinearities entering this procedure are entailed in the continuously changing transformation matrices between local and global systems (rotational effect of elements).

Two equations are of great importance for a nonlinear analysis: the equilibrium equations and the incremental form of the equilibrium equations. The condition of equilibrium for an element can be stated in terms of the virtual work principle

$$\int_V \sigma\delta\varepsilon dV - \int_{S_1} T_i \delta u_i dS = 0 \qquad (1)$$

For a beam element $\sigma$ is the axial stress, V the element volume, $T_i$ the surface traction which is prescribed on surface $S_1$, $\delta u_i$ are the virtual displacements and $\delta\varepsilon$ the corresponding virtual strain. Using the approach just described, Eq. (1) yields the small displacement (secant) stiffness relation, i.e. the equilibrium equation, referred to the local coordinate system in the current deformed configuration. Eq. (1) may very well account for nonlinear material effects.

By considering equilibrium of two configurations 1 and 2 of the element that are close to each other, an incremental form of the virtual work principle may be obtained

$$\int_V \Delta\sigma\delta\varepsilon dV + \int_V \sigma\delta\Delta\varepsilon dV - \int_{S_1} \Delta T_i \delta u_i dS = 0 \qquad (2)$$

where $\Delta$ denotes increment of quantities between the two configurations. In accordance with the previous description Eq. (2) has been linearized by neglecting the term $\int_V \Delta\sigma\delta\Delta\varepsilon dV$.

The reference frame for Eq. (2) is the local coordinate system in configuration 1, see Fig. 1. For a beam element the term $\delta\Delta\varepsilon$ may be obtained from the nonlinear strain term which includes the rotational effect $\frac{1}{2}(\frac{\partial w}{\partial x})^2$, so that

$$\delta\Delta\varepsilon = \delta[\tfrac{1}{2}(\frac{\partial w}{\partial x} + \frac{\partial \Delta w}{\partial x})^2 - \tfrac{1}{2}(\frac{\partial w}{\partial x})^2] = \delta(\frac{\partial w}{\partial x}) \frac{\partial \Delta w}{\partial x} \quad (3)$$

Equation (2) yields the socalled incremental or tangent stiffness relation which accounts for both nonlinear material properties and geometric effects (geometric stiffness on linearized form).

## Finite Element Model

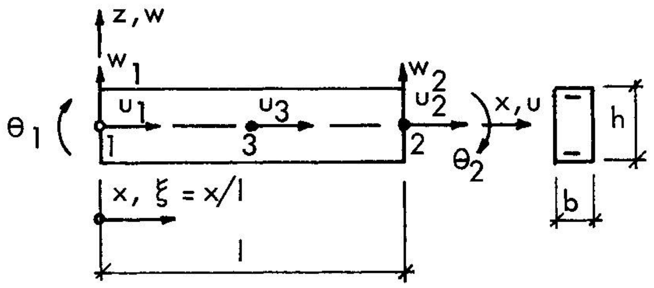


Fig.2. The beam element.

The finite element idealization of the beams is here based on a pure displacement model [1]. The axial displacement along the x-axis of a beam element is defined by

$$u_o = \mathbf{N}_u \mathbf{u} \quad (4)$$

where

$$\mathbf{N}_u = [\xi,\ 1-\xi,\ 4\xi(1-\xi)] \quad (5)$$

$$\mathbf{u} = [u_1,\ u_2,\ u_3]^T \quad (6)$$

The internal degree of freedom at the midplane, see Fig. 2, is introduced in order that the strain due to axial deformation be of the same degree as the strain due to flexure. The lateral displacement $w$ is defined by

$$w = \mathbf{N}_w \mathbf{w} \quad (7)$$

where

$$\mathbf{N}_w = [1-3\xi^2+2\xi^3, -\ell\xi(1-\xi)^2,\ 1-3(1-\xi)^2+2(1-\xi)^3, \ell\xi^2(1-\xi)] \quad (8)$$

$$\mathbf{w} = [w_1, \theta_1, w_2, \theta_2]^T \quad (9)$$

Adopting Kirchhoff's hypothesis, the strain at an arbitrary point within the beam element is given by

$$\varepsilon = \frac{du}{dx} = \mathbf{N}_{u,x}\mathbf{u} - z\mathbf{N}_{w,xx}\mathbf{w} \quad (10)$$

The comma denotes differentiation. The above model does not account for shear deformations.

Assuming that forces act only at the nodal points of an element, the element equilibrium equation is obtained by substitution of Eq. (10) into Eq. (1).

$$\int_V \sigma \begin{bmatrix} \mathbf{N}^T_{u,x} \\ -z\mathbf{N}^T_{w,xx} \end{bmatrix} dV = \begin{bmatrix} \mathbf{S}_u \\ \mathbf{S}_w \end{bmatrix} = \mathbf{S} \quad (11)$$

$\mathbf{S}$ is the nodal point force vector corresponding to the state of stress $\sigma$. The stress $\sigma$ is given by the current strain, see the next section.

The increment of the axial stress is related to the strain increment through the equation

$$\Delta\sigma = E_T\Delta\varepsilon \quad (12)$$

where $E_T$ is the current tangent modulus. By substitution of Eqs. (10) and (12) into Eq. (2), the incremental force-displacement relationship for the element is obtained

$$\left[\int_V E_T \begin{bmatrix} N_{u,x}^T N_{u,x}, & -zN_{u,x}^T N_{w,xx} \\ \text{symm.}, & z^2 N_{w,xx}^T N_{w,xx} \end{bmatrix} dV + N\int_\ell \begin{bmatrix} 0 & 0 \\ 0 & N_{w,x}^T N_{w,x} \end{bmatrix} dx\right] \begin{bmatrix} \Delta u \\ \Delta w \end{bmatrix} = \begin{bmatrix} \Delta S_u \\ \Delta S_w \end{bmatrix} = \Delta S \quad (13)$$

Here, N is the resulting axial force over the element cross section. The second term of Eq. (13) is the geometric contribution to the incremental force-displacement relationship. A similar incremental relationship for the total structure is obtained by transformation from the current local to the global coordinate system and using a standard assemblage process.

## Material properties

The method described herein allows for a general, nonlinear stress-strain relationship for both concrete and reinforcement. The concrete and the steel are assumed to be perfectly bonded.

In the computational procedure, it is assumed that there is a unique relationship between stresses and strains (total deformation formulation). The stress-strain curve for the concrete is identified by a set of discrete points, see Fig. 3. Linear interpolation between these points are used for intermediate values. The tangent modulus needed in Eq. (13) is given in a similar way by utilizing discrete tangent values from the experimental stress-strain curve. The tangent modulus may be negative. In tension the concrete is assumed to behave linearly up to a cracking strain $\varepsilon_{cr}$ beyond which the concrete has no strength. The computer program which was developed can also automatically generate the standard CEB-FIP design curve for concrete [7] (also used in the Norwegian building code NS 3473).

The material properties for the steel are obtained in a similar way as for the concrete by identifying discrete values from experimental curves.

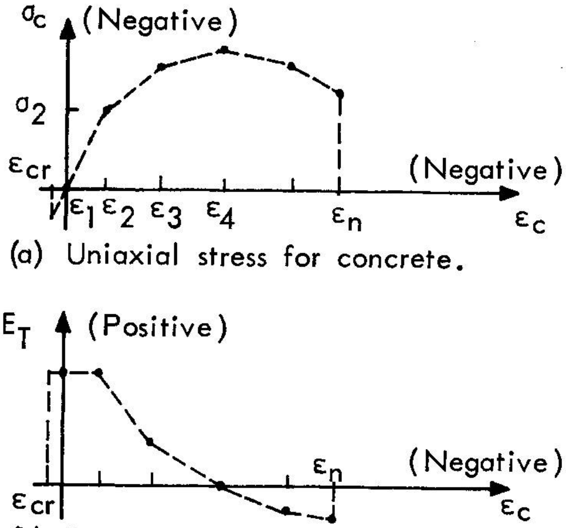

(a) Uniaxial stress for concrete.
(b) Tangent modulus for concrete

Fig.3. Material properties for concrete.

## Numerical solution

The major constituents in the solution process are the equilibrium equation (11) and its incremental form Eq. (13). These equations require integration to be carried out over the volume of the beam elements. A Gaussian quadrature scheme is adopted for this purpose. This integration is performed by utilization of 2 to 4 cross sections located at Gaussian points along the longitudinal axis of the beam element. Integration is also carried out over the height of each section employing Gaussian integration for stress points in the compression zone. The material properties at these points are obtained from diagrams like that of Fig. 3. The part of the tension zone where the strain exceeds the cracking limit is excluded from the integration. Several layers of reinforcement can also be accounted for.

The response of the structure during increasing external loading is basically determined by applying the external load in increments and by performing equilibrium iterations at each new level of loading. It may well happen that equilibrium of the structure is not satisfied after a new displacement vector has been obtained. The difference between the external forces acting on the structure and the assemblage of element force vectors from Eq. (11) give rise to a set of unbalanced forces. This residual force vector is utilized in a Newton-Raphson iteration in which the gradient matrix is supplied by Eq. (13). The iteration is terminated when the displacements have converged or material rupture has occured. The material properties at the integration points and the extension of the cracked zones are constantly updated during solution according to the current state of deformations. Also the local coordinate systems for the elements are steadily updated to account for the change in geometry of the frame.

The solution process is capable of proceeding beyond points of maximum carrying capacity of the structure. The load-steps automatically change sign after maximum point has been passed (reduction of external loading). This capability can be of great importance for determining the safety of a design. Further details on the solution procedure that is used may be found in Ref. [8].

## Numerical Examples

The present method will be illustrated by two numerical examples.

The first example is a hinged column subjected to eccentric axial loading, see Fig. 4. The steel reinforcement is symmetric and it is assumed to behave elastic-ideally plastic. Its modulus of elasticity is $E_s = 2.055 \cdot 10^5$ N/mm$^2$(29.2$\cdot 10^6$ psi) and its yield strength is $f_y = 461$ N/mm$^2$(65500 psi). The compressive stress-strain relationship of concrete is described by the standard CEB-FIP curve [7] with an ultimate strain of $\varepsilon_c = -0.0035$. The maximum compressive strength is taken as $f_c = 25.7$ N/mm$^2$(3660 psi) corresponding to 80 per cent of the cube strength. The tensile strenght of concrete is neglected. Half the total length of the column is divided into six beam elements. The axial loading is applied in 18 increments and an equilibrium iteration is carried out at each level of loading. Fig. 4 shows the load-deflection curve for the present analysis compared with test and analytical results from Ref. [6]. The results obtained agree closely with the two other curves. For all the curves the maximum point corresponds to an axial force of $N = 242$ kN (53.4 kips). To some extent, the discrepancy between the test curve and the analytical curves may be due to that the tensile strength has been set equal to zero. Fig. 5 shows a graph of the relationship between moment (M) and axial force (N) at the critical section of the column during deformation. The interaction diagram which represents material failure is also plotted in the figure. It is clearly demonstrated

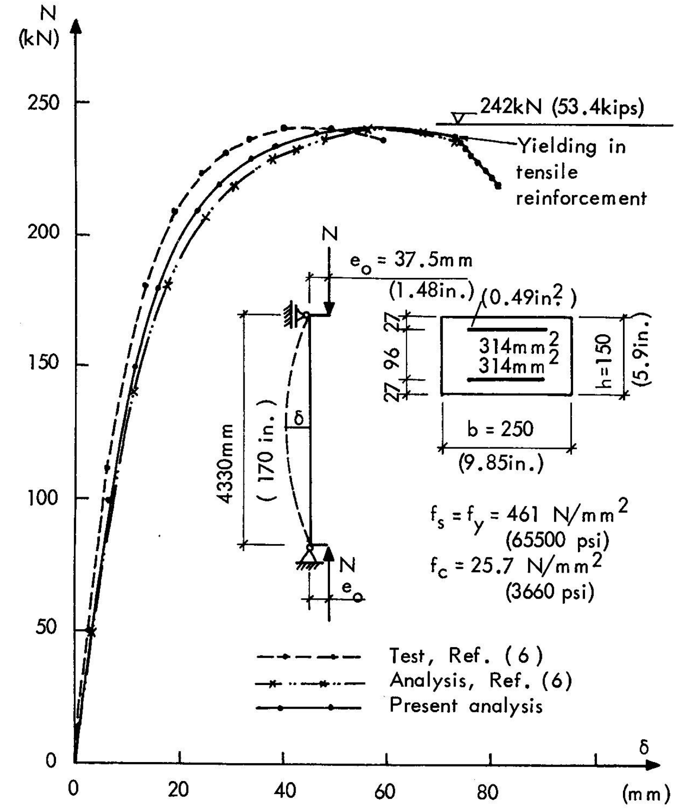


Fig.4. Load - deflection curves for column.

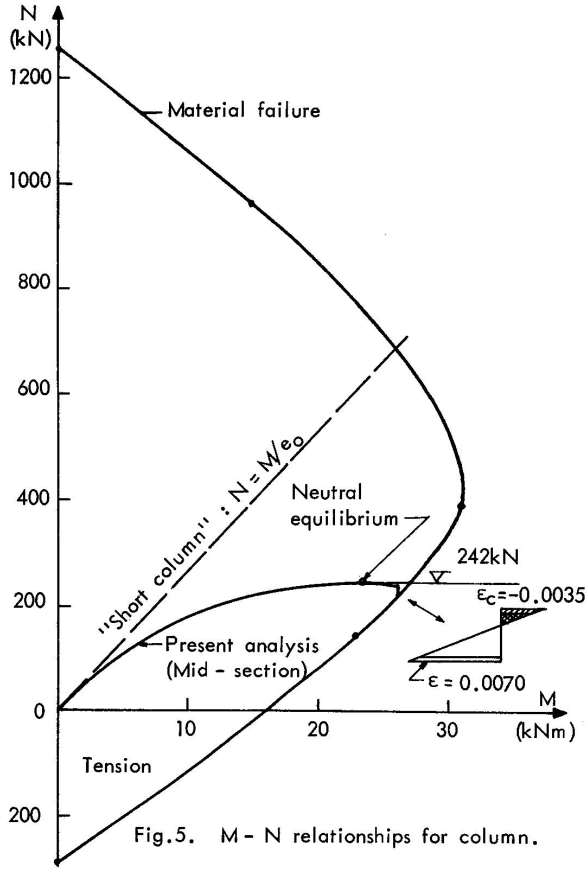


Fig.5. M - N relationships for column.

that the final collapse of the column occurs when the M-N curve of the column reaches the interaction diagram (failure envelope). The total solution time for this example was 18 CPU-seconds on a UNIVAC 1108 computer.

The second example is a $180^{\circ}$ hinged arch subjected to uniform hydrostatic pressure. Since no test data or alternative analytical results are available, the main purpose of this example is to demonstrate various capabilities of the present approach. The dimensions of the arch are given in Fig. 7. It is assumed to have a geometric imperfection defined by $e = e_o \sin 2\alpha$. The ultimate strain of the steel is taken as $\varepsilon_{su} = \varepsilon_y + 0.005 = 0.0069$. The arch is analyzed both as an unreinforced concrete structure with perfectly linear elastic material properties and as a reinforced concrete structure with nonlinear material properties. The shape of the nonlinear stress-strain relationship is assumed to be the same as for the previous example, and the numerical values are given in Fig. 6. The hydrostatic pressure is applied both as a conservative loading for which the original direction of the force is kept during deformation and as a nonconservative loading for which the water pressure always is acting perpendicular to the deformed configuration. The arch is divided into 12 equal elements.

The results obtained are shown in Figs. 6 and 7. In Fig. 6, the horizontal displacement of node 4, $u_{x4}$, is plotted against the load intensity p. Curve ② shows the load-displacement relationship for an elastic structure subjected to a nonconservative load. The curve approaches the critical load level for linearized buckling $p_{cr} = 3EI/R_o^3 = 418$ N/mm. A similar curve for conservative loading is marked ①. Curve ③ and ④ represent a reinforced concrete arch with conservative and nonconservative load, respectively. Curve ③ reaches its peak value at a load level of $p_{s3} \simeq 250$ N/mm. Material failure is reached at $p_{m3} \simeq 140$ N/mm $= 0.56\, p_{s3}$. The corresponding values for curve ④ are $p_{s4} \simeq 230$ N/mm and $p_{m4} \simeq 125$ N/mm $= 0.54\, p_{s4}$. The curves representing nonconservative load are located approximately 10 per cent lower than the corresponding curves representing conservative load. This demonstrates that practical design procedures ought to account for changes in the direction of loads. From Fig. 6 it may also be seen that the asymptotes of the elastic curves are located about 80 per cent higher than the maximum points of the corresponding reinforced concrete curves. Fig. 7 shows the relationship between moment (M) and axial force (N) at the critical section (node 4) for the reinforced concrete arch with conservative and nonconservative loading, respectively. Also the corresponding interaction diagram (failure envelope) is shown. The loading was applied in 11 to 22 load increments corresponding to a total solution time of 30 to 76 CPU-seconds on a UNIVAC 1108 computer.

## References

[1] ZIENKIEWICZ, O.C., *The Finite Element Method in Engineering Science*, McGraw-Hill, London (1971)

[2] ODEN, J.T., *Finite Elements of Nonlinear Continua*, McGraw-Hill, New York (1971)

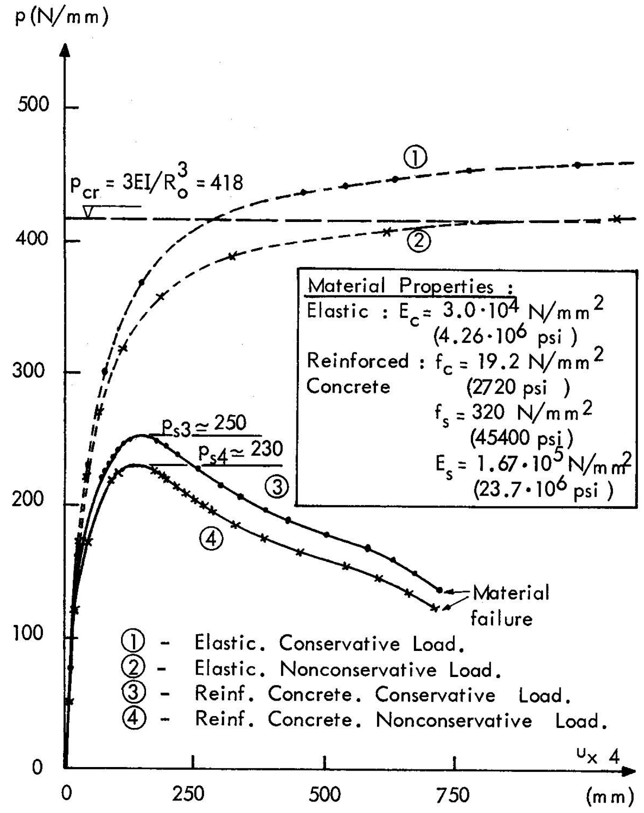

Fig.6. Load – deflection curves for arch. ( Horizontal displacement of node 4 )

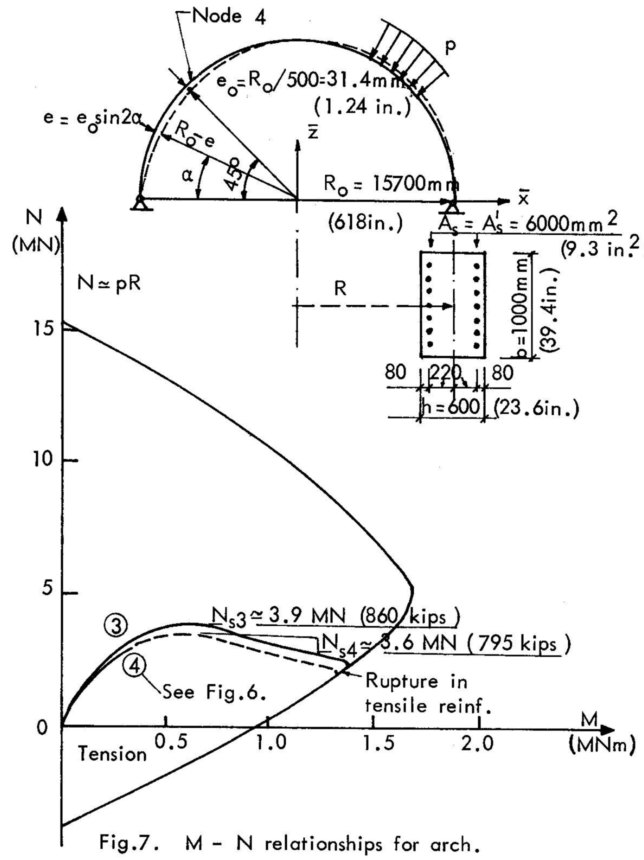

Fig.7. M – N relationships for arch.

[3] SCORDELIS, A.C., "Finite Element Analysis of Reinforced Concrete Structures", presented at the *June 1-2. 1972, Speciality Conference on the Finite Element Method in Civil Engineering*, Montreal, Canada.

[4] BERG, S., BERGAN, P.G., HOLAND, I., "Nonlinear Finite Element Analysis of Reinforced Concrete Plates", *Proceedings of the 2nd International Conference on Structural Mechanics in Reactor Technology*, Vol. M, Berlin, Sept. 1973.

[5] BLAAUWENDRAAD, Ir.J., "Realistic Analysis of Reinforced Concrete Framed Structures", *HERON*, Vol. 18, No. 4, 1972.

[6] AAS-JAKOBSEN, K.A., GRENACHER, M., *Berechnung unelastischer Rahmen nach der Theorie 2. Ordnung*, Bericht Nr. 45, Institut für Baustatik, ETH, Zürich, Januar 1973.

[7] CEB-FIP, *International Recommendations for the Design and Construction of Concrete Structures*, English Edition, June 1970.

[8] BERGAN, P.G., SØREIDE, T., "A Comparative Study of Different Numerical Solution Techniques as applied to a Nonlinear Structural Problem", *Computer Methods in Applied Mechanics and Engineering* 2 (1973) 185 - 201.

SUMMARY

The paper presents a method of nonlinear analysis for plane, reinforced concrete frames. Both geometric and material nonlinearities are accounted for. The method allows for incremental application of the external loads and the structural behaviour may be followed even beyond the point of maximum carrying capacity. The analysis is based on a finite element formulation in which the frames are modelled by small beam elements. The present method has proved to be very efficient and accurate.

RESUME

Ce rapport présente une méthode de calcul non-linéaire pour les cadres plans en béton armé. On tient compte des comportements non-linéaires et de la géométrie et du matériau. Cette méthode permet d'étudier le comportement d'une structure sous l'accroissement de la charge extérieure, même au-delà du point où la charge maximum est atteinte. Le calcul se base sur la méthode des éléments finis: les cadres sont considérés comme un assemblage de petits éléments de poutre. On a démontré que la méthode ci-dessus était efficace et exacte.

ZUSAMMENFASSUNG

Der Beitrag stellt eine Methode vor, mit welcher eine nichtlineare Berechnung ebener Stahlbetonrahmen möglich ist. Sowohl die geometrischen Nichtlinearitären als auch diejenigen der Baustoffe werden berücksichtigt. Die Methode gestattet stufenweises Aufbringen der äusseren Belastung, und das Verhalten lässt sich selbst über den Punkt der maximalen Tragfähigkeit hinaus verfolgen. Die Berechnung benützt die Methode der Finiten Elemente, wobei der Rahmen aus kleinen Balkenelementen zusammengesetzt wird. Die vorliegende Methode hat sich als sehr leistungsfähig und genau erwiesen.

Leere Seite
Blank page
Page vide